© 2020. Published by The Company of Biologists Ltd | Journal of Experimental Biology (2020) 223, jeb207472. doi:10.1242/jeb.207472

RESEARCH ARTICLE

Walking with added mass magnifies salient features of human foot energetics

Nikolaos Papachatzis[1], Philippe Malcolm[1], Carl A. Nelson[2] and Kota Z. Takahashi[1,*]

ABSTRACT

The human foot serves numerous functional roles during walking, including shock absorption and energy return. Here, we investigated walking with added mass to determine how the foot would alter its mechanical work production in response to a greater force demand. Twenty-one healthy young adults walked with varying levels of added body mass: 0%, +15% and +30% (relative to their body mass). We quantified mechanical work performed by the foot using a unified deformable segment analysis and a multi-segment foot model. We found that walking with added mass tended to magnify certain features of the foot's functions. Magnitudes of both positive and negative mechanical work, during stance in the foot, increased when walking with added mass. Yet, the foot preserved similar amounts of net negative work, indicating that the foot dissipates energy overall. Furthermore, walking with added mass increased the foot's negative work during early stance phase, highlighting the foot's role as a shock-absorber. During mid to late stance, the foot produced greater positive work when walking with added mass, which coincided with greater work from the structures spanning the midtarsal joint (i.e. arch). While this study captured the overall behavior of the foot when walking with varying force demands, future studies are needed to further determine the relative contribution of active muscles and elastic tissues to the foot's overall energy.

KEY WORDS: Biomechanics, Energy, Power, Multi-segment foot, Locomotion

INTRODUCTION

The human foot is composed of numerous anatomical structures that can independently produce different mechanical functions as they interact with the ground (Holowka and Lieberman, 2018). During stance phase, the forces propagate along the sole of the foot, which requires individual structures to adapt to a variety of functional behaviors, including energy dissipation, storage, return and/or generation. For example, the surrounding structures of the longitudinal arch (e.g. plantar fascia) can lengthen to store elastic energy during loading and return energy during unloading (Ker et al., 1987; Wager and Challis, 2016; McDonald et al., 2016; Stearne et al., 2016). Moreover, the foot's intrinsic muscles (e.g. abductor hallucis, flexor digitorum brevis) can actively control the longitudinal arch deformation by increasing their activation as a response to the applied load (Kelly et al., 2014). The windlass mechanism, which can help maintain the arched position of the foot, influences the energy storage within the foot (Welte et al., 2018). Beyond that, the viscoelastic fibroadipose tissue, such as the fat on the heel pad and under the metatarsal heads, can compress and dissipate energy during heel strike (Gefen et al., 2001) and push-off (Cavanagh, 1999), respectively. While there is a critical need to quantify the contribution of individual structures to human foot energetics, recent studies have also gained new insights from understanding the summed behavior of all foot structures during locomotion (Takahashi et al., 2017; Kelly et al., 2018; Zelik and Honert, 2018; Honert and Zelik, 2019).

When accounting for all structures within the human foot, these structures seemingly dissipate energy overall during level-ground steady-state walking (Takahashi et al., 2017) and running (Kelly et al., 2018; Bruening et al., 2018). In other words, despite the presence of muscles that can actively produce positive work and elastic structures (e.g. plantar fascia) that can return energy, the foot structures altogether perform more negative work than positive work (i.e. net negative work or net energy dissipation). Although the contributions of this net negative work performed by isolated foot structures are unclear, studying the net effect of the entire foot structures may reveal general principles that underlie the foot's functions during a variety of locomotion tasks. It has not been fully recognized and explained how the foot structures could alter their mechanical function as a unit with the aim of satisfying the various requirements of different locomotion tasks. Determining exactly when and where the foot's work production is manipulated remains a challenge, and improving such knowledge will help uncover the fundamental structure–function relationships that govern human locomotion.

Here, we used walking with added mass to increase the force demand of the foot and investigated how the foot could modulate mechanical functions. During walking with added mass, the musculotendon structures surrounding the hip, knee and ankle modulate their work production (Griffin et al., 2003). Similarly, the added mass could cause a variety of changes to the foot's mechanical behavior, and examining these changes may reveal insights regarding the foot's functional capacity. For example, when walking with greater force demand (i.e. greater levels of added mass), the human foot structures could hypothetically: (1) increase the magnitude of net negative work dissipation, which may highlight the foot's role of shock absorption (i.e. energy dissipation), (2) increase the positive work to generate net positive work, which may reveal the foot muscles' potential to actively produce work under greater force demand, or (3) increase similar magnitudes of positive and negative work and maintain roughly equal net work, which could indicate either that elastic structures play a prominent role in adapting to greater force demands of walking or that the muscles actively produced nearly equal amounts of positive and negative work. These scenarios may suggest that the added mass (i.e. increased force demand) could have a variety of mechanical consequences on foot function by magnifying the energetic output of some structures more than others.

[1]Department of Biomechanics, University of Nebraska at Omaha, Omaha, NE 68182, USA. [2]Department of Mechanical and Materials Engineering, University of Nebraska–Lincoln, Lincoln, NE 68588, USA.

*Author for correspondence (ktakahashi@unomaha.edu)

P.M., 0000-0003-4110-4167; K.Z.T., 0000-0003-1731-480X

Received 19 May 2019; Accepted 11 May 2020

The purpose of this study was to determine how the human foot modulates mechanical work production when walking with varying levels of increased force demand (i.e. added mass). We expected that walking with increasing levels of added mass (i.e. greater force demand) would exaggerate the foot's role towards energy dissipation. Specifically, we hypothesized that the net work performed by the foot would be more negative, and part of this negative work would happen during early stance phase, highlighting the foot's role as a shock absorber. We based these predictions on existing knowledge. First, there is fibroadipose tissue underneath the heel that has viscoelastic properties (Gefen et al., 2001), which could dissipate more energy when subjected to greater magnitudes of force during heel strike. Second, the elastic structures, like the plantar fascia, can store and return energy with a small hysteresis (Ker et al., 1987), and therefore may not change the net work output during stance irrespective of the force magnitude. Barring any major changes in foot muscle activations, we expected that the net effect of all foot structures would magnify the amount of energy dissipation while walking with increased levels of force demand. In fact, a recent study involving human running found that the foot becomes more net dissipative when increasing running speeds (Kelly et al., 2018), providing more support for our hypotheses. The findings of the present study may not only contribute to how humans adapt to various force demands during locomotion, but may also form a basis for comparison for other species – in particular, to identify anatomical features that are prominent in humans that may be lacking in other species, leaving humans well suited for producing and/or dissipating energy as the foot interacts with the external environment.

MATERIALS AND METHODS

Participants

A total of 21 healthy young adults (6 females, 15 males; age=24.14±2.88 years; height=173.61±6.67 cm; mass=83.17±20.26 kg; means±s.d.) volunteered to participate in this experiment. Participants were free of cardiac and neurological pathologies (such as arrhythmia, heart attack and stroke) and free of any musculoskeletal or pathological problems (such as osteoarthritis, bone fractures, etc.). All data collected in this study were in accordance with the protocol approved by the local Institutional Review Board. Each subject provided written informed consent before participating in the experiment.

Experimental protocol

Participants completed barefoot walking in three loading conditions of added mass relative to their body mass: 0% (i.e. no added body mass), +15% and +30% (Fig. 1). The participants walked over a 10 m walkway equipped with five force plates (AMTI Inc., Watertown, MA, USA) and the order of added mass conditions was randomized for each participant. To ensure minimum contact time deviations across the three conditions, the walking speed was targeted at 1.25 m s^{-1}. Walking speed was controlled using timing gates and verbal feedback was provided to the participants. Only clean foot strikes were accepted, where the entire foot came in complete contact within the force plate's borders. For each subject, we analyzed approximately five stance phase data series (e.g. 3–7 per subject) for each walking condition. For each subject, the stance data were averaged for each variable (e.g. negative, positive and net work).

Participants wore a tight-fitting 'wrestling' suit. This suit promoted accurate and consistent placement of retro-reflective markers. The retro-reflective markers were placed directly on the skin and the surface of the wrestling suit using double-sided tape at specific anatomical locations on each participant (Bruening et al., 2012a,b). These include bony landmarks of the feet, ankles and knees. Marker clusters were used to track the movement of the shank, thigh and pelvis.

Multi-segment foot model

The selection of the landmarks was adapted from the work of Bruening et al. (2012a,b) and divided the foot into three segments: hindfoot, forefoot and hallux. The hindfoot and forefoot segments were separated by the midtarsal joint, defined by the midpoint between the markers that were placed on the navicular and cuboid bones (NV and CU markers in Fig. 1). The midtarsal joint was modeled as a six degree-of-freedom (DOF) joint. The forefoot and hallux segments were separated by the first metatarsophalangeal joint. The joint center was defined as the midpoint between the first metatarsal head marker (H1 in Fig. 1) and the vertical projection on the floor. The metatarsophalangeal joint was modeled as a two DOF joint (permitting dorsiflexion/plantarflexion and adduction/abduction) using inverse kinematics (Bruening et al., 2012a). The hindfoot and the shank were separated by the ankle joint, which was defined as the midpoint between the markers on the medial and lateral malleoli. The ankle joint was modeled as a six DOF joint.

Added mass

Participants carried symmetrical loads (+15% and +30% of added body mass, metal weights=2.5 kg) secured closely at the posterior and the anterior areas of the trunk. The symmetrical distribution of the loads reduced the muscular activity required to balance asymmetrically positioned loads, such as with backpacks (Bobet and Norman, 1984). To accomplish this, participants wore a weighted vest, which has a smaller effect on the anterior–posterior center of mass location compared with heavy backpacks (Datta and Ramanathan, 1971).

Analysis

Lower limb mechanics

An eight-infrared camera motion analysis system (Raptor-4S, Motion Analysis Corp., Mountain View, CA, USA) was used to capture the position of the retro-reflective markers relative to the global reference system of the laboratory at 180 Hz. Five force plates collected ground reaction force data at 1080 Hz. Data processing and analyses were conducted using Cortex motion analysis software (Motion Analysis Corp.), Visual3D (C-motion, Germantown, MD, USA) and MATLAB R2018a (MathWorks, Natick, MA, USA). To minimize the error in the center of pressure (COP) estimates, we used the CalTester tool to assess the accuracy of the force platform when used in conjunction with the motion capture system (Holden et al., 2003), where we found an average error of 2.04±1.35, 1.34±1.23 and 1.36±0.91 mm (mean±s.d. of the five force plates) for the three axes. Before all processing and analysis, raw data from marker trajectories and ground reaction forces were filtered by applying a second-order dual-pass low-pass Butterworth filter of 6 Hz for kinematic data, and 25 Hz for kinetic data. A 20 N threshold for the vertical ground reaction force defined the start and the end time for each stance phase of walking.

Distal-to-hindfoot (i.e. structures of the entire foot) mechanical power and work

We quantified the mechanical power and work done by all structures distal to the hindfoot's center of mass (i.e. structures of the entire foot), using a unified deformable segment analysis (Takahashi et al., 2012).

Journal of Experimental Biology (2020) 223, jeb207472. doi:10.1242/jeb.207472

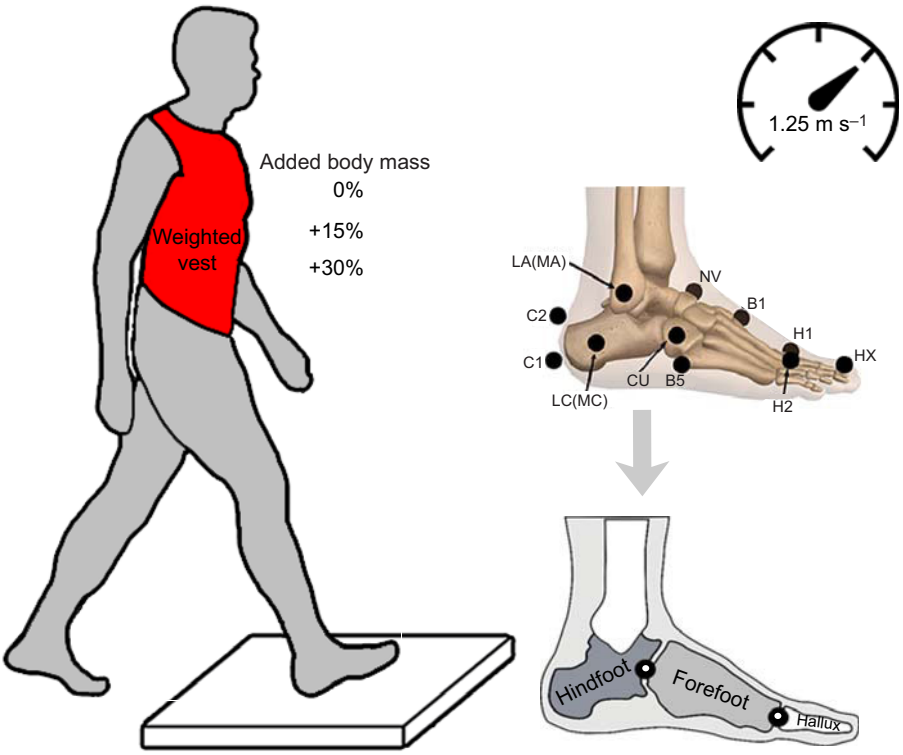

Fig. 1. Participants (*N*=21) completed barefoot over-ground walking at 1.25 m s^{-1} in three randomized loading conditions (0% or no added body mass, +15%, and +30% of added body mass) wearing a weighted vest. We quantified the mechanical power that is due to all structures distal to the hindfoot. The selection of the landmarks was adapted from the work of Bruening et al. (2012a,b) and the foot was divided into three segments: hindfoot, forefoot and hallux. The hindfoot and forefoot segments were separated by the midtarsal joint (six degrees of freedom). The joint was defined as the midpoint between the navicular (NV) and cuboid (CU) markers. The H2 marker (located halfway between the second and third metatarsal heads) defined the forefoot distal end by vertically projecting the H2 marker by half the distance to the floor. The H1 marker (located on the superior aspect of the first metatarsal head) defined the proximal end of the hallux by vertically projecting the H1 marker by half the distance to the floor. As the ground reaction forces propagate underneath the foot, the structures of the foot either move (e.g. muscles, metatarsal–phalangeal joints, etc.) or deform (e.g. soft tissues), which displaces the center of pressure (COP) with respect to the hindfoot's center of mass. The displacement of the COP with respect to the hindfoot segment center of mass describes the overall mechanical behavior of all the structures distal to the hindfoot (i.e. entire foot). LA, lateral malleolus; LM, medial malleolus; C2, superior apex of calcaneus; C1, apex of calcaneal tuberosity; LC, lateral calcaneus; MC, medial calcaneus; NV, medial prominence of navicular bone; CU, lateral centroid of cuboid bone; B1, medial aspect of 1st metatarsal base; B5, lateral aspect of 5th metatarsal base; H1, superior aspect of 1st metatarsal head; H2, midway between 2nd and 3rd metatarsal heads; HX, centroid of hallux nail.

This analysis captures the total mechanical contribution of the heel pad deformation, midtarsal joint, metatarsophalangeal joint, hallux segment and all the other structures that the foot contains (e.g. foot arches, plantar aponeurosis, surrounding muscles and tendons, etc.) (Takahashi et al., 2017). This analysis can also be thought of as power/work of the 'hindfoot relative to the ground' (Zelik and Honert, 2018).

The displacement of the COP relative to the hindfoot's center of mass is defined by the vector $\vec{r}_{\mathrm{cop/H}}$. The center of mass location for the hindoot (and for the other foot segments: forefoot and hallux) was consistent with the model defined by Bruening et al. (2012a,b). The mass among the three segments was partitioned in the same ratios as their respective volumes, assuming each segment was a geometric solid with uniform density (Bruening et al., 2012a,b). The total distal velocity ($\vec{V}_{\mathrm{H\_dist}}$) is produced by the movement of all the structures distal to the hindfoot's center of mass. These movements can be caused by the foot arches, the plantar aponeurosis, the surrounding muscles and tendons within the foot, or soft tissue deformation. $\vec{V}_{\mathrm{H\_dist}}$ is quantified using Eqn 1:

$$\vec{V}_{\mathrm{H\_dist}} = \vec{V}_{\mathrm{H\_cm}} + (\vec{\omega}_{\mathrm{H}} \times \vec{r}_{\mathrm{cop/H}}), \quad (1)$$

where $\vec{V}_{\mathrm{H\_cm}}$ is the translational velocity of the hindfoot's center of mass, and $\vec{\omega}_{\mathrm{H}}$ is the angular velocity of the hindfoot. The distal-to-hindfoot power is quantified using Eqn 2:

$$P = \vec{F}_{\mathrm{gnd}} \cdot \vec{V}_{\mathrm{H\_dist}} + (\vec{M}_{\mathrm{free}} \cdot \vec{\omega}_{\mathrm{H}}), \quad (2)$$

where $\vec{F}_{\mathrm{gnd}}$ is the ground reaction force and $\vec{M}_{\mathrm{free}}$ is the free moment. This analysis assumes that the contribution of mass and inertial effects are zero (Takahashi et al., 2012). The analysis also does not account for the radial velocity component of the vector $\vec{r}_{\mathrm{cop/H}}$, as inclusion of this term can lead to a power imbalance in a foot segment (McGibbon and Krebs, 1998). We quantified the negative and positive mechanical work over the entire stance phase by integrating the positive portions of the mechanical power data over time to calculate positive work, and the negative portions to calculate negative work.

Sub-dividing stance phases

We temporally partitioned the distal-to-hindfoot (i.e. structures of the entire foot) work production into two sub-phases of stance: (1) when the COP was posterior to the midtarsal joint during early stance (or when the COP was underneath the hindfoot segment), and (2) when the COP was anterior to the midtarsal joint during mid to late stance (or when the COP was underneath the forefoot or hallux segments). To determine the timing in which the COP crosses

Journal of Experimental Biology (2020) 223, jeb207472. doi:10.1242/jeb.207472

anteriorly to the midtarsal joint, we compared the anterior–posterior positions of the COP relative to the midtarsal joint in the laboratory coordinate system. Based on a prior study (Bruening and Takahashi, 2018), we expected that the work performed during the first sub-phase (when the COP is posterior to the midtarsal joint) would include contributions from structures underneath the hindfoot, such as the heel pad, and contributions from tissues crossing the midtarsal joint. During the second sub-phase (when the COP is anterior to the midtarsal), the work estimates would include contributions from structures surrounding the longitudinal arch and toes, such as the plantar fascia and foot muscles.

Midtarsal joint and distal-to-forefoot work

The multi-segment foot model used in this study (Bruening et al., 2012a) enabled additional analyses of power and work contributions from the midtarsal joint and structures distal to the forefoot's center of mass, similar to an approach entailed in prior studies (Takahashi et al., 2017; Bruening et al., 2018; Riddick et al., 2019). A prior study found that the summation of the midtarsal joint and distal-to-forefoot powers are nearly equivalent to the distal-to-hindfoot power in mid to late stance phase (Takahashi et al., 2017). The midtarsal joint power was quantified using a full six DOF approach (Buczek et al., 1994; Zelik et al., 2015) in which the joint moment and joint force were assumed to be zero when the COP was posterior to the midtarsal joint (Bruening and Takahashi, 2018). Although a portion of the midtarsal joint moment and negative work during early stance could be missed with this approach, a prior study found that the positive work estimates from this method are accurate (Bruening and Takahashi, 2018).

To quantify power and work contributions from all structures distal to the forefoot's center of mass, we used a unified deformable segment analysis (Takahashi et al., 2017). The mathematical approach is nearly identical to the distal-to-hindfoot power described earlier, but with Eqns 1 and 2 expressed relative to the forefoot segment's center of mass. Distal-to-forefoot power and work were quantified only when the COP was anterior to the midtarsal joint. We have verified that the summation of midtarsal joint and distal-to-forefoot powers would be nearly equal to distal-to-hindfoot power (Fig. S1).

From the multi-segment foot model, we determined whether foot kinematics were altered when walking with added mass, by quantifying the peak midtarsal joint angle and the total angular displacement (range of motion) about the dorsiflexion/plantarflexion, inversion/eversion and abduction/adduction axes of the midtarsal joint (forefoot relative to hindfoot), and about the dorsiflexion/plantarflexion and abduction/adduction axes of the metatarsophalangeal joint (hallux relative to forefoot). For the midtarsal joint, we defined the peak dorsiflexion and adduction angles as the maximum angles during stance, while we defined the peak inversion angle as the last local maximum during stance. We defined dorsiflexion and plantarflexion angular displacement as the difference from heel strike to the corresponding peak angles, and we defined inversion, eversion, abduction and adduction angular displacements as the difference between the angles at heel strike to the angles at the time of peak dorsiflexion. For the metatarsophalangeal joint, peak angles for dorsiflexion and adduction were defined as the maximum angles during the stance phase. Metatarsophalangeal joint angular displacement for dorsiflexion/plantarflexion was defined as the difference between

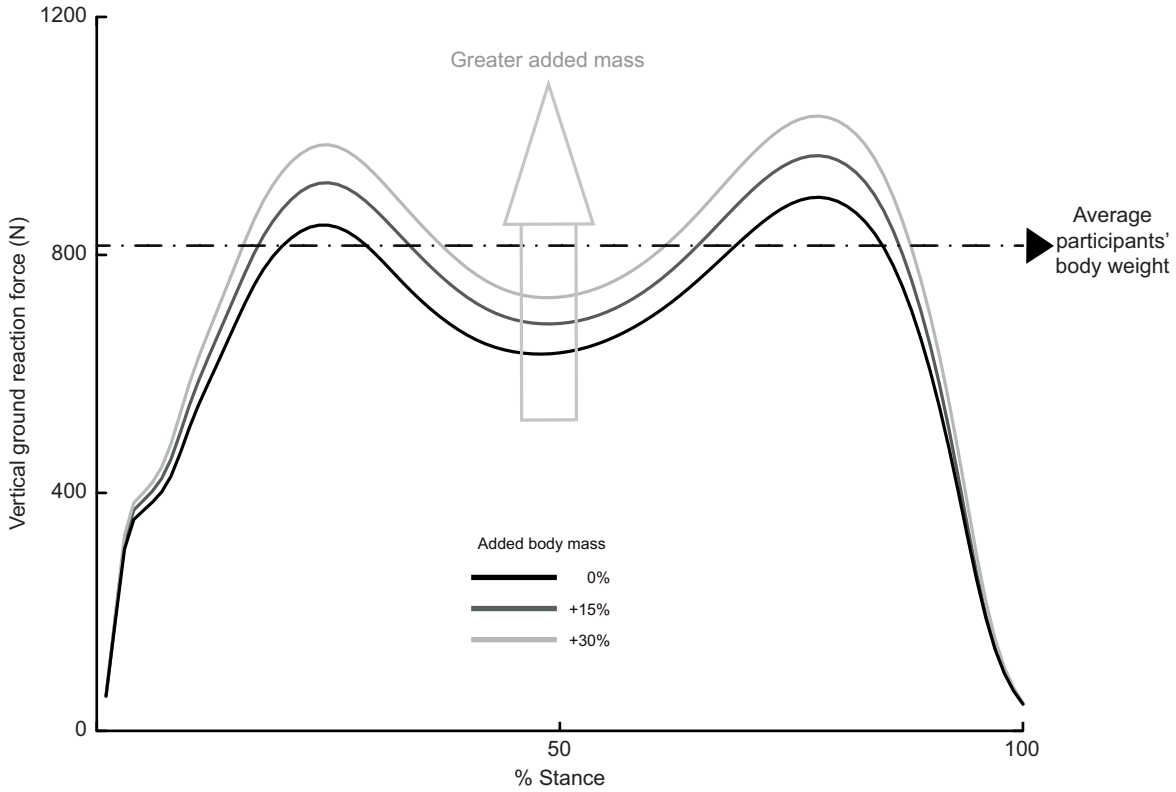

Fig. 2. Average vertical ground reaction forces during stance phase of different walking conditions of all subjects (*N*=21). Each line represents the average vertical ground reaction force of all participants for each walking condition (0% or no added body mass, +15, and +30% of added body mass). The horizontal dashed–dotted line represents the average body weight of all participants. Walking with added mass increased vertical ground reaction forces.

Journal of Experimental Biology (2020) 223, jeb207472. doi:10.1242/jeb.207472

the maximum and minimum angles, while angular displacement for abduction/adduction was computed as the difference between the angle at heel strike and the maximum angle.

Statistical analyses

All dependent variables were checked for normality. All mechanical work-based calculations were normalized by subjects' biological mass (not including the added mass). Because we used added mass as an experimental model that illustrates the potential of the foot structures to do work during demanding force tasks, we chose biological mass as a way of normalization to express how much additional work the structures of the foot would perform when walking with additional loads. In other words, our normalization method will quantify the relative changes in work (per biological body mass) when external mass is added to the body. We have also provided our work-based dependent variables with additional normalization techniques as supplementary material (see Tables S1–S5), including un-normalized values and normalized by total mass (biological plus added mass of the weighted vests). In order to determine the effect of the added mass on the dependent variables (negative, positive and net mechanical work), one-factor (three levels of added mass conditions) repeated-measures

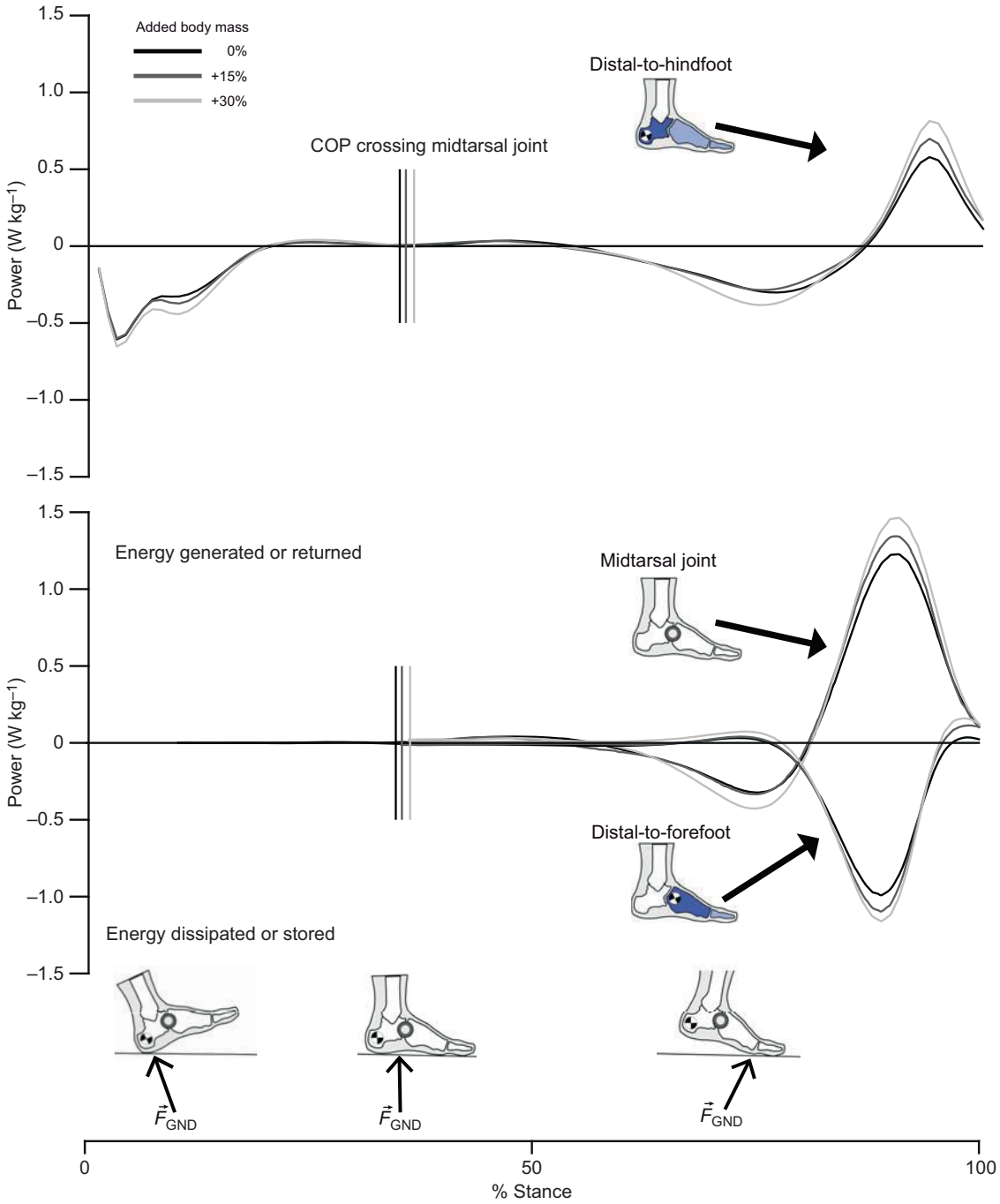

Fig. 3. Total power produced by the structures distal-to-hindfoot (i.e. entire foot), midtarsal joint and distal-to-forefoot during stance. Each line represents the average mechanical power during stance from all participants (N=21) for each walking condition (0% or no added body mass, +15%, and +30% of added body mass). The vertical lines denote the instance when the center of pressure (COP) moved anteriorly to the midtarsal joint. F_{gnd}, ground reaction force.

Journal of Experimental Biology (2020) 223, jeb207472. doi:10.1242/jeb.207472

ANOVAs were used (IBM SPSS Statistics 24, SPSS Inc., Chicago, IL, USA). When a significant main effect was found, a Bonferroni *post hoc* analysis was conducted for pair-wise comparisons. The significance level was set to α=0.05.

RESULTS

Ground reaction forces

Walking with added mass increased the vertical ground reaction forces during walking, thus confirming that the force demand on the foot structures increased (Fig. 2). In addition, the targeted walking speed did not significantly differ across the added mass conditions (P=0.262).

Distal-to-hindfoot power/work during stance

Across the three walking conditions (0% or no added body mass, +15%, and +30% of added body mass), the structures of the foot produced varying levels of mechanical power and work (Figs 3 and 4). Added mass had a significant effect on the magnitude of positive (P<0.001) and negative (P=0.034) work. The positive work production increased by 22% between 0% and +30% of added body mass conditions (P<0.001). The magnitude of negative work increased by 14% between 0% and +30% of added mass conditions (P=0.023), and by 15% between +15% and +30% of added mass conditions (P=0.027). Overall, the structures of the foot produced net negative work across all the walking conditions. However, there was no significant effect of added mass on net work (P=0.236; Fig. 4).

When the COP was underneath the hindfoot (posterior to the midtarsal joint)

Added mass had a significant effect on the negative (P=0.024) and net work (P=0.035), but not on the magnitude of positive work (P=0.298; Fig. 5). The magnitude of negative work increased by 18% between 0% and +30% of added mass conditions (P=0.013). Overall, the structures underneath the hindfoot produced net negative work across all of the walking conditions. The magnitude of net negative work increased by 19% between 0% and +30% of added body mass conditions (P=0.021).

When the COP was underneath the forefoot and hallux (anterior to the midtarsal joint)

Added mass had a significant effect on the magnitude of positive work (P<0.001). However, there was no significant effect of added mass on the magnitude of the negative (P=0.157) or net work (P=0.187). The positive work production increased by 23% between 0% and +30% of added body mass conditions (P<0.001). Overall, the structures underneath the forefoot/hallux produced nearly equal amounts of positive and negative work, resulting in net work close to zero.

Midtarsal joint power/work

Added mass had a significant effect on the magnitude of midtarsal joint positive work (P<0.001) and net work (P=0.014; Fig. 5). However, there was no significant effect of added mass on the magnitude of the negative work (P=0.220). The positive work production increased by 10% between 0% and +15% of added body mass conditions (P<0.001), by 17% between 0% and +30% of added body mass conditions (P<0.001) and by 7% between 15% and +30% (P=0.028). Overall, the structures surrounding the midtarsal joint produced net positive work across all the walking conditions. The net work increased by 23% between 0% and +30% of added body mass conditions (P=0.025).

Distal-to-forefoot power/work

Added mass had a significant effect on the magnitude of distal-to-forefoot positive work (P=0.002). The positive work production increased by 23% between 0% and +15% of added body mass conditions (P=0.034), and by 36% between 0% and +30% of added body mass conditions (P=0.006). Overall, the

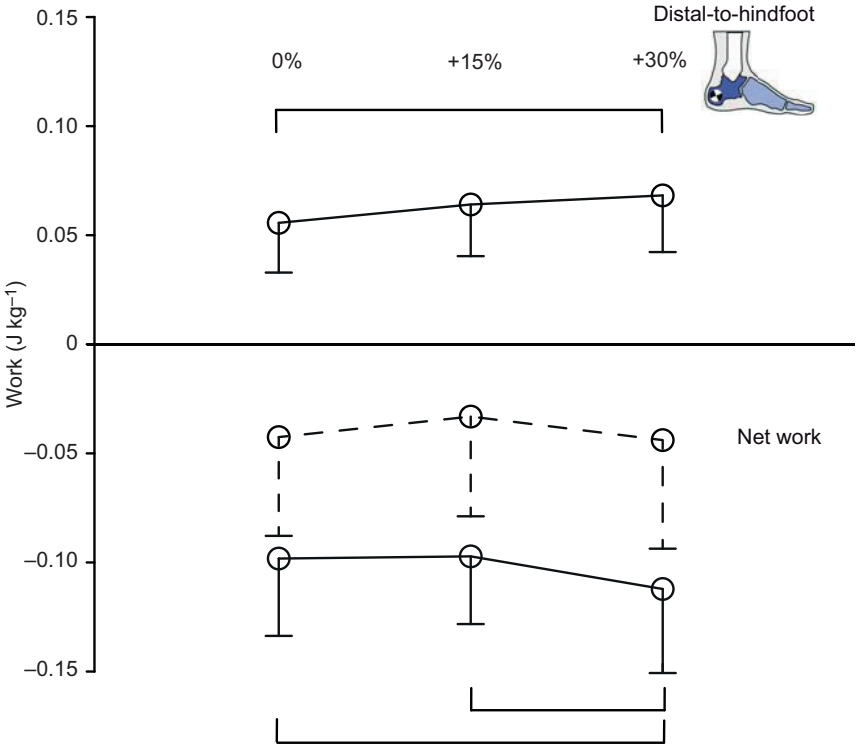

Fig. 4. During the entire stance phase, walking with added mass significantly increased the foot's magnitudes of positive (P<0.001) and negative work (P=0.034), but not net work (dashed lines) (P=0.236). Significant pair-wise comparisons are denoted via the square brackets (N=21).

Journal of Experimental Biology (2020) 223, jeb207472. doi:10.1242/jeb.207472

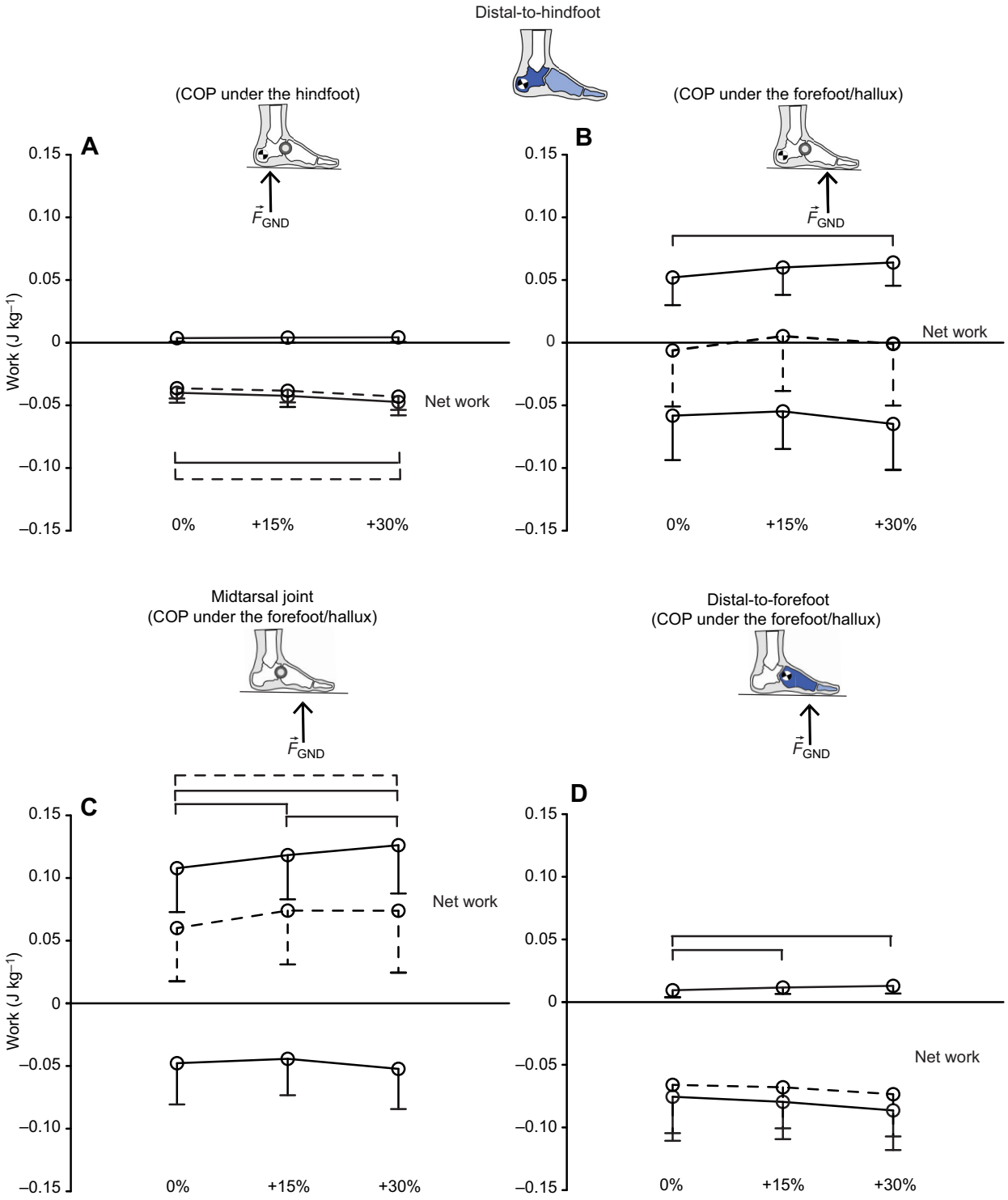

Fig. 5. Sub-dividing the foot work production into stance phases of stance. (A) When the center of pressure (COP) was under the hindfoot, walking with added mass had a significant effect on the magnitude of distal-to-hindfoot negative (P=0.024) and net negative work (P=0.035), but not on positive work (P=0.298). (B) When the COP was under the forefoot/hallux, walking with added mass significantly increased the magnitude of distal-to-hindfoot positive work (P<0.001), but not negative work (P=0.157) or net work (P=0.187). (C) Added mass had a significant effect on the magnitude of midtarsal joint positive work (P<0.001) and net work (P=0.014), but not on negative work (P=0.220). (D) Added mass had a significant effect on the distal-to-forefoot positive work (P=0.002) but not on the negative (P=0.055) and net work (P=0.218). Net work is denoted by the dashed lines. Significant pair-wise comparisons are denoted via the square brackets for positive work, and via dashed square brackets for net work (N=21).

structures of the foot produced net negative work across all the walking conditions. However, there was no significant effect of added mass on negative work (P=0.055) or net work (P=0.218; Fig. 5).

DISCUSSION

In this study, we used walking with added mass to increase the force demand on the foot to determine how the foot could modulate mechanical energy. We hypothesized that walking

Journal of Experimental Biology (2020) 223, jeb207472. doi:10.1242/jeb.207472

with increasing levels of added mass would increase the magnitude of foot energy dissipation (i.e. net work would be more negative) overall during stance, and more negative work would be performed early in the stance phase. Our results partially supported our hypotheses that walking with added mass increased the magnitude of foot's net negative work during the early stance phase in which the COP was underneath the hindfoot; however, overall, the foot preserved similar amounts of net negative work per stance. The increased foot negative work during early stance was offset by increased positive work during push-off. The relative percent

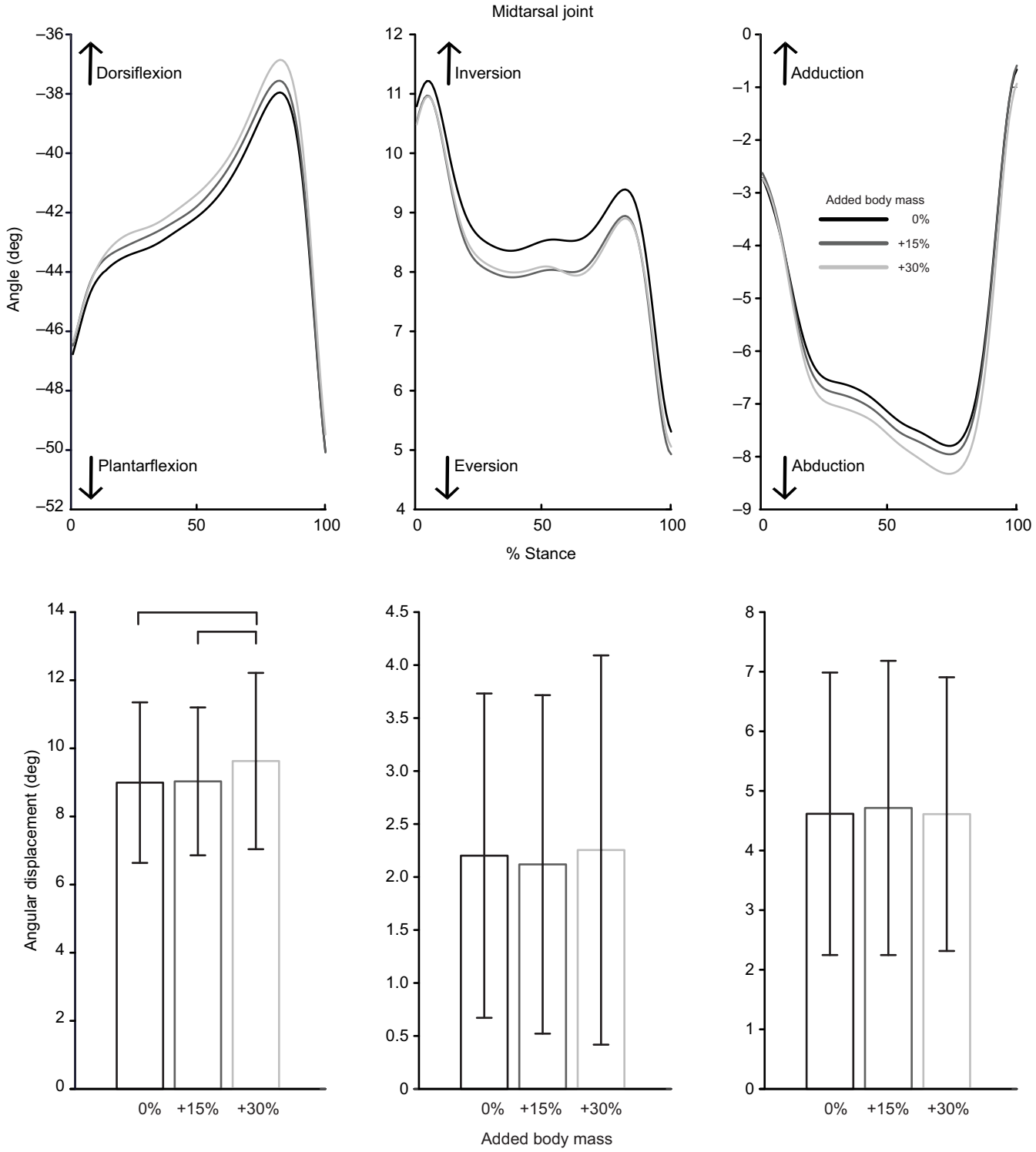

Fig. 6. Added mass affected the angular displacement of the midtarsal joint. Across the added mass conditions, we found significant differences in the angular displacement in the midtarsal joint for the dorsiflexion/plantarflexion axis (from heel strike to peak dorsiflexion) (P=0.002), but not in the angular displacement for the inversion/eversion and adduction/abduction axes (P=0.788 and P=0.676, respectively). Additionally, there was a significant increase in peak dorsiflexion and peak abduction of the midtarsal joint (P<0.001 and P=0.023, respectively; N=21). Significant pair-wise comparisons are denoted via the square brackets.

Journal of Experimental Biology (2020) 223, jeb207472. doi:10.1242/jeb.207472

increase in work was slightly lower than the percentage of added mass carried – for example, the magnitude of foot's negative and positive work (during entire stance) normalized to the biological body mass increased by 14% and 22%, respectively, when walking with 30% added mass. Such findings may indicate that the active and/or passive structures responsible for producing work have limits in their capacity to increase work when faced with greater force demand, especially for negative work. Overall, the net dissipative behavior of the human foot during stance is consistent with previous studies in walking (Takahashi et al., 2017) and running (Kelly et al., 2018; Bruening et al., 2018).

Our findings confirmed the shock absorption function of the human foot immediately following ground contact. When the COP was underneath the hindfoot, which coincided with the first ∼40% of stance, negative work done during this phase accounted for ∼41% of the total negative work during the entire stance phase. The magnitude of net work after heel strike during unloaded walking (−2.988 J or −0.036 J kg^{-1} per stance) is similar to the values reported in a prior study in human walking of −3.8 J (Baines et al., 2018). Walking with +30% added mass further increased the foot's energy loss up to −3.476 J (−0.043 J kg^{-1}) of net work. Although our analysis cannot precisely isolate which individual structures surrounding the hindfoot are responsible for energy dissipation, we speculate that a large portion could be attributed to heel pad deformation. For example, Wearing et al. (2014) used dynamic radiographs and found that the heel pad can dissipate approximately 1.0 J of energy per stance. The difference between this radiographic-based estimate and our estimates (−2.988 J or −0.036 J kg^{-1}) could

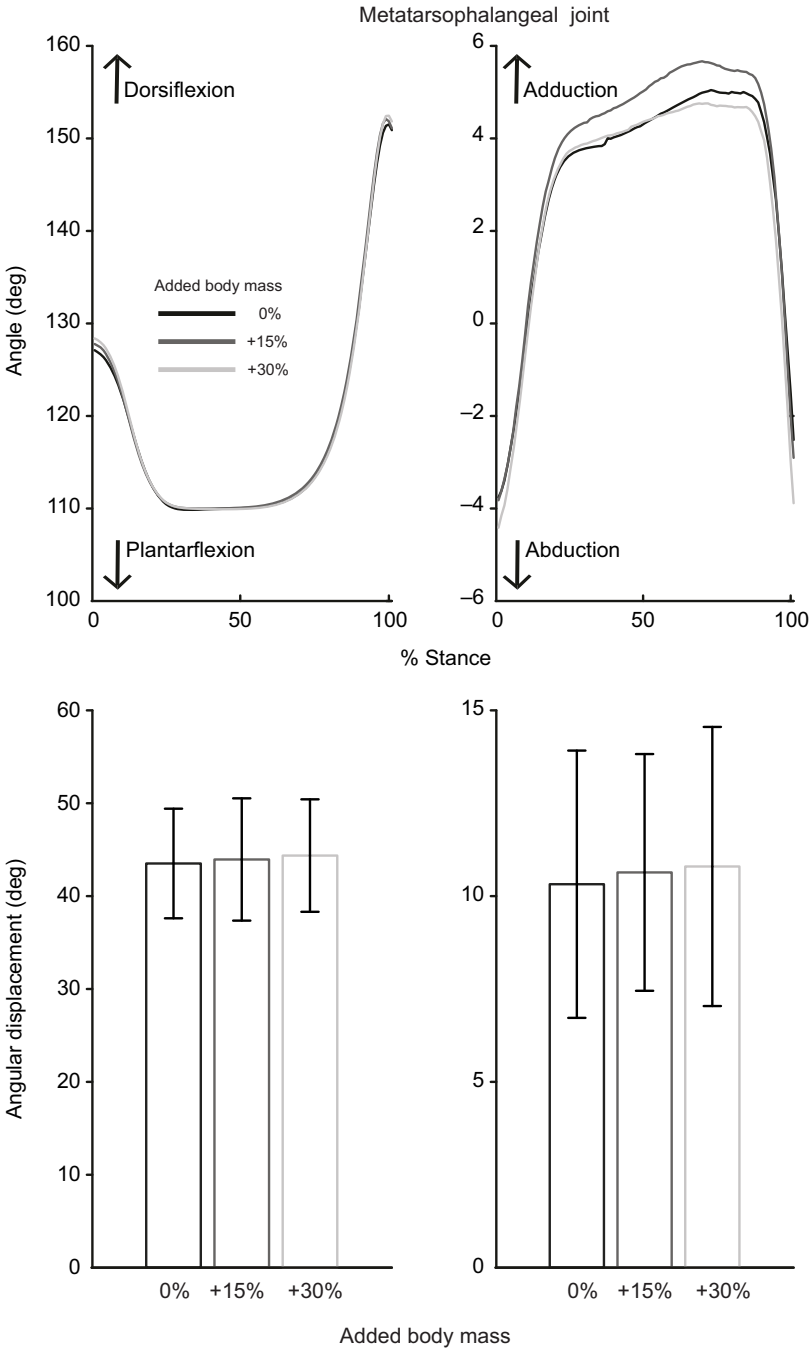

Fig. 7. Added mass did not affect the angular displacement of the metatarsophalangeal joint. Across the added mass conditions, we found no significant differences in the angular displacement in the metatarsophalangeal joints for the dorsiflexion/plantarflexion and adduction/abduction axes (P=0.184 and P=0.355, respectively). Additionally, no significant differences were found for the peak dorsiflexion and peak abduction (P=0.095 and P=0.602, respectively; N=21).

be due to several factors. First, our study involved a slightly faster walking speed (1.25 m s^{-1}) compared with the Wearing et al. (2014) study (1.0 m s^{-1}). Second, their study measured the force and displacement of the heel pad only in the vertical direction (Wearing et al., 2014), whereas our distal-to-hindfoot work estimates include vertical as well as shear components. And third, our distal-to-hindfoot estimates likely include other sources besides the heel pad deformation. By the time the COP crosses anteriorly to the midtarsal joint (~40% of stance), there is sufficient loading on the forefoot segment (Bruening et al., 2010), which could compress the soft tissue underneath the segment. In fact, a recent study quantified distal-to-forefoot work using only the forces applied to the forefoot/hallux segments and showed non-negligible negative powers occurring in the first ~40% of stance (Takahashi et al., 2017). Besides that, it is possible that tissues crossing the midtarsal joint (e.g. plantar fascia and muscle–tendon structures spanning the arch) could contribute to some of the early stance negative work. A prior study found that the midtarsal joint could contribute to some of the early stance negative work (roughly 0.007 J kg^{-1}) during walking (Bruening and Takahashi, 2018), which would equate to roughly 18% of the negative work during early stance estimated in the present study. Future work may be needed to combine imaging-based methods (e.g. radiographic or ultrasound) and motion capture-based techniques to determine the precise contributions of the work done after heel strike by structures surrounding the hindfoot.

During mid to late stance after the COP passed anterior to the midtarsal joint, the foot produced nearly equal amounts of negative work (−4.771 J or −0.058 J kg^{-1} per stance) and positive work (4.389 J or 0.0520 J kg^{-1}), resulting in net work close to zero (−0.382 J or −0.006 J kg^{-1}). During this phase of stance (last ~60% of stance), the hindfoot segment is mostly unloaded (Bruening et al., 2010) so that the work produced during this period would likely represent contributions from structures spanning the midtarsal joints or tissues surrounding the forefoot/hallux. Although elastic structures such as the plantar fascia can contribute to both positive and negative work (Ker et al., 1987; Wager and Challis, 2016; McDonald et al., 2016; Stearne et al., 2016), we speculate that the elastic mechanism alone does not explain all or most of the work production in the foot. A recent study using computational modeling found that the plantar fascia could store roughly 3.1 J of energy per stance during running (Wager and Challis, 2016), which is less than the 4.389 J (0.0520 J kg^{-1}) of positive work estimated in our walking study. It is expected that the plantar fascia contributions would be less than 3.1 J (Wager and Challis, 2016) during walking owing to smaller forces acting on the foot. Although it is possible that other elastic structures besides plantar fascia (e.g. tendons of extrinsic foot muscles) could contribute to work production, it is likely that active muscles contribute to a portion of the overall work production.

Walking with added mass revealed additional insights about the foot's work production during mid to late stance phase. During this phase, the foot increased positive work production, which also coincided with greater positive work done by structures crossing the midtarsal joint. Although the mechanisms of this enhanced positive work are currently unclear, we have several speculations. First, the enhanced positive work could occur owing to energy stored (earlier in stance) and returned from elastic structures such as the plantar fascia. To test this idea, we performed secondary analyses of midtarsal and metatarsophalangeal joint kinematics (Figs 6 and 7). Across the added mass conditions, we found significant differences in angular displacement (from heel strike to peak dorsiflexion) in the midtarsal joint (P=0.002) but not in the metatarsophalangeal joint (P=0.184) for the dorsiflexion/plantarflexion axis. In addition, there was no significant increase in the angular displacement kinematics in the midtarsal joint for the inversion/eversion and abduction/adduction axes (P=0.788 and P=0.676, respectively). In addition, there was a significant increase in peak dorsiflexion/plantarflexion and peak abduction/adduction of the midtarsal joint (P<0.001 and P=0.023, respectively), but not for the peak dorsiflexion/plantarflexion and peak abduction/adduction of the metatarsophalangeal joint (P=0.095 and P=0.602, respectively). Finally, no significant differences were observed in angular displacement joint kinematics for the abduction/adduction axis of the metatarsophalangeal joint (P=0.355). The greater dorsiflexion peak of the midtarsal joint could indicate greater stretch of the plantar fascia; however, a more detailed model-based estimate of plantar fascia length would be needed to confirm this idea. Another plausible explanation for the greater positive work when walking with added mass may be active muscles. A recent study has found that the intrinsic foot muscles (e.g. flexor digitorum brevis and abductor hallucis) can modulate their activation to influence work production relative to the mechanical requirement of the task (Riddick et al., 2019). Although the joint/segment-based analyses presented in this study cannot parse out individual muscle contributions, further experiments that integrate model-based computations, *in-vivo* imaging and fine wire electromyography may be needed to reconcile the exact work contributions.

Our findings from human feet may form a basis for future comparisons with other species. Human walking is typically characterized by a habitual heel strike, which may contribute to human calcaneus morphology that may be absent in non-heel-striking primates. For example, the calcaneus of the great apes lacks the lateral plantar process, which could explain how apes may not attenuate impact forces as effectively as the human foot (Holowka and Lieberman, 2018). Our study confirmed the shock absorption function of the human foot immediately following ground contact. Furthermore, the longitudinal arch of humans is distinct from other primates (Holowka and Lieberman, 2018), which could affect how the foot performs work during locomotion. Understanding how morphological differences among humans and other primates affect the foot's ability to adapt to various force and work demands may provide future insights regarding evolution of upright and bipedal locomotion.

Conclusions

Our study revealed that the human foot could magnify mechanical energy output in response to walking with greater force demand (i.e. added mass). Magnitudes of negative and positive mechanical work during stance increased in the foot when walking with added mass, but preserved similar amounts of net negative work. Walking with added mass also magnified the amount of negative work done by the foot immediately after heel strike, highlighting its role as a shock absorber. During mid to late stance, the foot produced greater positive work when walking with added mass, possibly indicating greater active muscle involvement.

Acknowledgements

The authors thank Jeffrey M. Patterson for experimental assistance.

Competing interests

The authors declare no competing or financial interests.

Author contributions

Conceptualization: N.P., K.Z.T.; Methodology: N.P., K.Z.T.; Data curation: N.P.; Writing - original draft: N.P.; Writing - review & editing: N.P., K.Z.T.; Visualization: N.P.; Supervision: P.M., C.A.N., K.Z.T.; Funding acquisition: K.Z.T.

Funding

This project was supported by the University of Nebraska Collaboration Initiative, the Center for Research in Human Movement Variability of University of Nebraska at Omaha, and the National Institutes of Health (P20GM109090). The funders had no role in study design, data collection and analysis, decision to publish, or preparation of the manuscript. Deposited in PMC for release after 12 months.

Supplementary information

Supplementary information available online at
http://jeb.biologists.org/lookup/doi/10.1242/jeb.207472.supplemental

References

Baines, P. M., Schwab, A. L. and Van Soest, A. J. (2018). Experimental estimation of energy absorption during heel strike in human barefoot walking. *PLoS ONE* **13**, e0197428. doi:10.1371/journal.pone.0197428

Bobet, J. and Norman, R. W. (1984). Effects of load placement on back muscle activity in load carriage. *Eur. J. Appl. Physiol. Occup. Physiol.* **53**, 71-75. doi:10.1007/BF00964693

Bruening, D. A. and Takahashi, K. Z. (2018). Partitioning ground reaction forces for multi-segment foot joint kinetics. *Gait Posture* **62**, 111-116. doi:10.1016/j.gaitpost.2018.03.001

Bruening, D. A., Cooney, K. M., Buczek, F. L. and Richards, J. G. (2010). Measured and estimated ground reaction forces for multi-segment foot models. *J. Biomech.* **43**, 3222-3226. doi:10.1016/j.jbiomech.2010.08.003

Bruening, D. A., Cooney, K. M. and Buczek, F. L. (2012a). Analysis of a kinetic multi-segment foot model. Part I: Model repeatability and kinematic validity. *Gait Posture* **35**, 529-534. doi:10.1016/j.gaitpost.2011.10.363

Bruening, D. A., Cooney, K. M. and Buczek, F. L. (2012b). Analysis of a kinetic multi-segment foot model part II: kinetics and clinical implications. *Gait Posture* **35**, 535-540. doi:10.1016/j.gaitpost.2011.11.012

Bruening, D. A., Pohl, M. B., Takahashi, K. Z. and Barrios, J. A. (2018). Midtarsal locking, the windlass mechanism, and running strike pattern: a kinematic and kinetic assessment. *J. Biomech.* **73**, 185-191. doi:10.1016/j.jbiomech.2018.04.010

Buczek, F. L., Kepple, T. M., Siegel, K. L. and Stanhope, S. J. (1994). Translational and rotational joint power terms in a six degree-of-freedom model of the normal ankle complex. *J. Biomech.* **27**, 1447-1457. doi:10.1016/0021-9290(94)90194-5

Cavanagh, P. R. (1999). Plantar soft tissue thickness during ground contact in walking. *J. Biomech.* **32**, 623-628. doi:10.1016/S0021-9290(99)00028-7

Datta, S. R. and Ramanathan, N. L. (1971). Ergonomic comparison of seven modes of carrying loads on the horizontal plane. *Ergonomics* **14**, 269-278. doi:10.1080/00140137108931244

Gefen, A., Megido-Ravid, M. and Itzchak, Y. (2001). In vivo biomechanical behavior of the human heel pad during the stance phase of gait. *J. Biomech.* **34**, 1661-1665. doi:10.1016/S0021-9290(01)00143-9

Griffin, T. M., Roberts, T. J. and Kram, R. (2003). Metabolic cost of generating muscular force in human walking: insights from load-carrying and speed experiments. *J. Appl. Physiol.* **95**, 172-183. doi:10.1152/japplphysiol.00944.2002

Holden, J. P., Selbie, W. S. and Stanhope, S. J. (2003). A proposed test to support the clinical movement analysis laboratory accreditation process. *Gait Posture* **17**, 205-213. doi:10.1016/S0966-6362(02)00088-7

Holowka, N. B. and Lieberman, D. E. (2018). Rethinking the evolution of the human foot: insights from experimental research. *J. Exp. Biol.* **221**, jeb174425. doi:10.1242/jeb.174425

Honert, E. C. and Zelik, K. E. (2019). Foot and shoe responsible for majority of soft tissue work in early stance of walking. *Hum. Movement Sci.* **64**, 191-202. doi:10.1016/j.humov.2019.01.008

Kelly, L. A., Cresswell, A. G., Racinais, S., Whiteley, R. and Lichtwark, G. (2014). Intrinsic foot muscles have the capacity to control deformation of the longitudinal arch. *J. R. Soc. Interface* **11**, 20131188. doi:10.1098/rsif.2013.1188

Kelly, L. A., Cresswell, A. G. and Farris, D. J. (2018). The energetic behaviour of the human foot across a range of running speeds. *Sci. Rep.* **8**, 10576. doi:10.1038/s41598-018-28946-1

Ker, R. F., Bennett, M. B., Bibby, S. R., Kester, R. C. and Alexander, R. M. N. (1987). The spring in the arch of the human foot. *Nature* **325**, 147. doi:10.1038/325147a0

McDonald, K. A., Stearne, S. M., Alderson, J. A., North, I., Pires, N. J. and Rubenson, J. (2016). The role of arch compression and metatarsophalangeal joint dynamics in modulating plantar fascia strain in running. *PLoS ONE* **11**, e0152602. doi:10.1371/journal.pone.0152602

McGibbon, C. A. and Krebs, D. E. (1998). The influence of segment endpoint kinematics on segmental power calculations. *Gait Posture* **7**, 237-242. doi:10.1016/S0966-6362(97)00041-6

Riddick, R., Farris, D. J. and Kelly, L. A. (2019). The foot is more than a spring: human foot muscles perform work to adapt to the energetic requirements of locomotion. *J. R. Soc. Interface* **16**, 20180680. doi:10.1098/rsif.2018.0680

Stearne, S. M., McDonald, K. A., Alderson, J. A., North, I., Oxnard, C. E. and Rubenson, J. (2016). The foot's arch and the energetics of human locomotion. *Sci. Rep.* **6**, 19403. doi:10.1038/srep19403

Takahashi, K. Z., Kepple, T. M. and Stanhope, S. J. (2012). A unified deformable (UD) segment model for quantifying total power of anatomical and prosthetic below-knee structures during stance in gait. *J. Biomech.* **45**, 2662-2667. doi:10.1016/j.jbiomech.2012.08.017

Takahashi, K. Z., Worster, K. and Bruening, D. A. (2017). Energy neutral: the human foot and ankle subsections combine to produce near zero net mechanical work during walking. *Sci. Rep.* **7**, 15404. doi:10.1038/s41598-017-15218-7

Wager, J. C. and Challis, J. H. (2016). Elastic energy within the human plantar aponeurosis contributes to arch shortening during the push-off phase of running. *J. Biomech.* **49**, 704-709. doi:10.1016/j.jbiomech.2016.02.023

Wearing, S. C., Hooper, S. L., Dubois, P., Smeathers, J. E. and Dietze, A. (2014). Force-deformation properties of the human heel pad during barefoot walking. *Med. Sci. Sports Exerc.* **46**, 1588-1594. doi:10.1249/MSS.0000000000000281

Welte, L., Kelly, L. A., Lichtwark, G. A. and Rainbow, M. J. (2018). Influence of the windlass mechanism on arch-spring mechanics during dynamic foot arch deformation. *J. R. Soc. Interface* **15**, 20180270. doi:10.1098/rsif.2018.0270

Zelik, K. E. and Honert, E. C. (2018). Ankle and foot power in gait analysis: Implications for science, technology and clinical assessment. *J. Biomech.* **75**, 1-12. doi:10.1016/j.jbiomech.2018.04.017

Zelik, K. E., Takahashi, K. Z. and Sawicki, G. S. (2015). Six degree-of-freedom analysis of hip, knee, ankle and foot provides updated understanding of biomechanical work during human walking. *J. Exp. Biol.* **218**, 876-886. doi:10.1242/jeb.115451

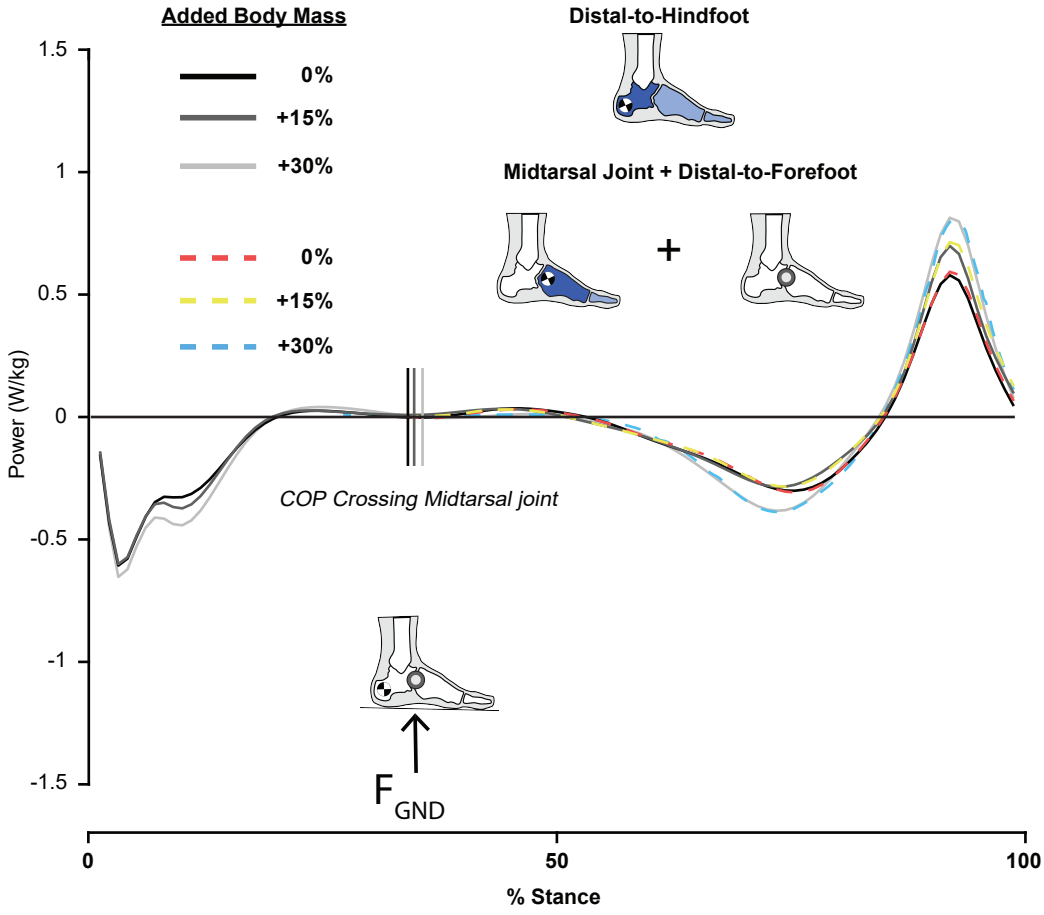

Fig. S1. Mechanical power (N=21) from subareas of the foot: distal-to-hindfoot (solid lines) and summed midtarsal joint and distal-to-forefoot (dashed lines). After the center-of-pressure (COP) moves anterior to the midtarsal joint (denoted by the vertical lines), the magnitude of distal-to-hindfoot power is similar to the summation of midtarsal joint and distal-to-forefoot powers.

Table S1: Distal-to-Hindfoot Work during Stance

		Un-normalized (J)	Body Mass (J/kg)	*Body Mass + Added Mass* (J/kg)
	Added Mass	**mean ± std.d**		
Negative Work	**%0**	-8.0549 ± 3.5831*	-0.0982 ± 0.0354**	-0.0982 ± 0.0355
	%15	-8.1254 ± 3.8319^{+}	-0.0972 ± 0.0310^{++}	-0.0865 ± 0.0273
	%30	-9.2261 ± 4.2079$^{*,+}$	-0.1122 ± 0.0379$^{**,++}$	-0.0885 ± 0.0299
Positive Work	**%0**	4.6847 ± 2.2115$^{¥,╫}$	0.0557 ± 0.0228$^{¥¥}$	0.0557 ± 0.0228
	%15	5.3558 ± 2.2739$^{¥}$	0.0641 ± 0.0237	0.0571 ± 0.0213
	%30	5.7480 ± 2.6823$^{╫}$	0.0682 ± 0.0260$^{¥¥}$	0.0538 ± 0.0204
Net Work	**%0**	-3.3702 ± 3.9143	-0.0425 ± 0.0453	-0.0425 ± 0.0453
	%15	-2.7696 ± 4.2325	-0.0331 ± 0.0457	-0.0294 ± 0.0406
	%30	-3.4780 ± 4.6964	-0.0439 ± 0.0498	-0.0347 ± 0.0392

* $p = 0.029$ || $^{+}p = 0.013$ || $^{**}p = 0.023$ || $^{++}$ $p = 0.027$ || $^{¥}p = 0.032$ || $^{╫}$ $p < 0.001$ || $^{¥¥}p < 0.001$

Table S2: Distal-to-Hindfoot Work when COP was posterior to midtarsal joint

		Un-normalized (J)	Body Mass (J/kg)	*Body Mass + Added Mass* (J/kg)
	Added Mass		**mean ± std.d**	
Negative Work	**%0**	-3.2841±0.9121*	-0.0400±0.0079+	-0.0400±0.0079
	%15	-3.4870±0.8901	-0.0424±0.0089	-0.0378±0.0081
	%30	-3.8335±0.7988*	-0.0473±0.0106+	-0.0378±0.0086
Positive Work	**%0**	0.2957±0.2264	0.0036±0.0028	0.0036±0.0028
	%15	0.3398±0.3470	0.0041±0.0040	0.0036±0.0035
	%30	0.3571±0.3288	0.0043±0.0036	0.0034±0.0029
Net Work	**%0**	-2.9884±0.9121**	-0.0363±0.0082++	-0.0363±0.0082
	%15	-3.1472±0.8668	-0.0384±0.0093	-0.0342±0.0085
	%30	-3.4763±0.7583**	-0.0431±0.0106++	-0.0340±0.0085

* $p = 0.006$ || + $p = 0.013$ || ** $p = 0.011$ || ++ $p = 0.021$

Table S3: Distal-to-Hindfoot Work when COP was anterior to midtarsal joint

		Un-normalized (J)	Body Mass (J/kg)	*Body Mass + Added Mass* (J/kg)
	Added Mass		**mean ± std.d**	
Negative Work	**%0**	-4.7708±3.4361	-0.0582±0.0354	-0.0582±0.0354
	%15	-4.6389±3.4015	-0.0548±0.0300	-0.0487±0.0264
	%30	-5.3926±3.9707	-0.0648±0.0367	-0.0512±0.0288
Positive Work	**%0**	4.3890±2.1484$^{*,+}$	0.0520±0.0221**	0.0520±0.0221
	%15	5.0159±2.1225*	0.0600±0.0219	0.0535±0.0197
	%30	5.3909±2.5230^{+}	0.0640±0.0242**	0.0504±0.1900
Net Work	**%0**	-0.3818±3.9544	-0.0062±0.0447	-0.0062±0.0447
	%15	0.3770±4.0165	0.0052±0.0438	0.0048±0.0390
	%30	-0.0017±4.7473	-0.0009±0.0493	-0.0007±0.0387

* p = 0.040 || $^{+}$p <0.001 || **p < 0.001

Table S4: Midtarsal 6DOF Joint Work during Stance

		Un-normalized (J)	Body Mass (J/kg)	*Body Mass + Added Mass* (J/kg)
	Added Mass		**mean ± std.d**	
Negative Work	**%0**	-4.0015±3.2081	-0.0478±0.0338	-0.0478±0.0338
	%15	-3.8525±3.3856	-0.0443±0.0290	-0.0393±0.0255
	%30	-4.3935±3.4278	-0.0523±0.0321	-0.0413±0.0253
Positive Work	**%0**	9.0485±3.7998^{++}	0.1078±0.0350$^{++,¥}$	0.1078±0.0350$^{¥¥}$
	%15	9.8870±3.7135**,*	0.1183±0.0353$^{++,ǂ}$	0.1053±0.0314^{ǂǂ}
	%30	10.5160±3.8066^{+**}	0.1262±0.0385$^{¥,ǂ}$	0.0995±0.0304$^{¥¥,ǂǂ}$
Net Work	**%0**	5.0470±3.5946$^{●,♦}$	0.0600±0.0425$^{●●}$	0.0600±0.0425
	%15	6.0345±3.5088$^{●}$	0.0740±0.0430	0.0660±0.0384
	%30	6.1231±4.1247$^{♦}$	0.0739±0.0494$^{●●}$	0.0582±0.03884

* p = 0.001 || $^{+}$p < 0.001 || **p = 0.039 || $^{++}$ p < 0.001 || $^{¥}$p < 0.001 || ^{ǂ} p = 0.028 || $^{¥¥}$p = 0.029 || ^{ǂǂ} p = 0.040 ||$^{●}$ p = 0.041||$^{♦}$ p = 0.028 || $^{●●}$ p = 0.025

Table S5: Distal-to-Forefoot Work during Stance

		Un-normalized (J)	Body Mass (J/kg)	*Body Mass + Added Mass* (J/kg)
	Added Mass		**mean ± std.d**	
Negative Work	**%0**	-6.1855±3.1207	-0.0755±0.0352	-0.0755±0.0352
	%15	-6.5815±2.9982*	-0.0769±0.0297	-0.0709±0.0263
	%30	-7.1175±3.0964*	-0.0864±0.0316	-0.0682±0.0250
Positive Work	**%0**	0.8085±0.5474$^{**,+}$	0.0095±0.0057$^{++,¥}$	0.0095±0.0057
	%15	0.9920±0.5826 **	0.0117±0.0052^{++}	0.0104±0.0046
	%30	1.1270±0.7161^{+}	0.0129±0.0061$^{¥}$	0.0102±0.0048
Net Work	**%0**	-5.3765±3.3617	-0.0660±0.0385	-0.0660±0.0385
	%15	-5.5895±3.1781	-0.0680±0.0328	-0.0605±0.0290
	%30	-5.9905±3.1358	-0.0735±0.0337	-0.0580±0.0267

* p = 0.025 || $^{+}$p = 0.009 || **p = 0.013 || $^{++}$ p = 0.034 || $^{¥}$p = 0.006